



Diffusion of organic anions in clay-rich mediaeffect of porosity exclusion on retardation

R.H. Dagnelie, S. Rasamimanana, V. Blin, J. Radwan, E. Thory, J-C. Robinet, G. Lefevre

► To cite this version:

R.H. Dagnelie, S. Rasamimanana, V. Blin, J. Radwan, E. Thory, et al.. Diffusion of organic anions in clay-rich mediaeffect of porosity exclusion on retardation. Chemosphere, Elsevier, 2018, 10.1016/j.chemosphere.2018.09.064 . cea-02339780

HAL Id: cea-02339780

<https://hal-cea.archives-ouvertes.fr/cea-02339780>

Submitted on 5 Nov 2019

HAL is a multi-disciplinary open access archive for the deposit and dissemination of scientific research documents, whether they are published or not. The documents may come from teaching and research institutions in France or abroad, or from public or private research centers.

L'archive ouverte pluridisciplinaire **HAL**, est destinée au dépôt et à la diffusion de documents scientifiques de niveau recherche, publiés ou non, émanant des établissements d'enseignement et de recherche français ou étrangers, des laboratoires publics ou privés.

Diffusion of organic anions in clay-rich media:
effect of porosity exclusion on retardation

R.V.H. Dagnelie^(a,*), S. Rasamimanana^(a), V. Blin^(a), J. Radwan^(a),
E. Thory^(a), J.-C. Robinet^(b), G. Lefèvre^(c)

^(a)DEN-Service d'Etude du Comportement des Radionucléides (SECR),
CEA, Université Paris-Saclay, F-91191 Gif-sur-Yvette, France

^(b) Andra, R&D Division, parc de la Croix Blanche, 92298, Châtenay-Malabry, France

^(c)PSL Research University, Chimie ParisTech-CNRS, Institut de Recherche de Chimie Paris,
11 rue Pierre et Marie Curie, F-75005 Paris, France

* Corresponding author: R.V.H. Dagnelie, romain.dagnelie@cea.fr, Tel: +33 (0)1 69 08 50 41

Highlights

- 1 Retarded diffusion of organic anions was studied in Callovo-Oxfordian claystone
- 2 Charge and or steric effects lead to strongly reduced apparent porosity for carboxylic acids
- 3 This exclusion lowers simultaneously porosity, effective diffusion and retardation
- 4 A correction factor is proposed with a retardation collapse below a threshold: $\varepsilon_a/\varepsilon < b$
- 5 A methodology is proposed to evaluate retardation of organic anions in claystones

Abstract

The adsorption of solutes in porous rocks and soils is known to induce retardation during transport. We studied the case of diffusion of organic anions in a clay rich media, for which a discrepancy was previously observed between adsorption measured by batch and diffusion experiments. Organic anions display an affinity with clay and oxides surfaces leading to adsorption. However, they are subject to a partial exclusion from porosity ($\epsilon_a < \epsilon$), because of steric and charge effects. We evaluated the possible correlation between the decrease of accessible porosity and a decrease of diffusive retardation. An empirical correction factor was proposed to explain the difference between maximum and apparent adsorption, respectively measured by batch and diffusion experiments. This correction was evaluated for Callovo-Oxfordian clay rock and used to interpret 15 diffusion experiments. A reasonable agreement was observed between adsorption isotherms from batch and corrected values from diffusion experiments. A low diffusivity of organic species in Callovo-Oxfordian was confirmed, with D_e values ranging between 0.5 and $7 \cdot 10^{-12} \text{ m}^2 \text{ s}^{-1}$, indicating anion exclusion. Still a significant retardation was observed for species such as oxalate, citrate or α -isosaccharinate. This retardation factor decreases with accessible porosity, with a threshold value observed when $\epsilon_a/\epsilon < 0.65$. This feature has strong implications for estimation of migration parameters of solutes in the environment. The proposed methodology would be suitable for other media with charged surfaces such as cementitious materials or oxisoils.

1. Introduction

Organic molecules are widely studied in environmental sciences such as pedology, geology or marine chemistry. Among them, organic pollutants such as anthropogenic organic matter (AOM) can be potentially released from hazardous waste and migrate through geological rock formation or soils (Duarte et al., 2018). AOM refers to a wide range of compounds, including polar and apolar molecules, ionic and neutral molecules. The ionic polar molecules are highly soluble in water and more mobile in soils and rocks (Schaffer and Licha, 2015). The neutral (poly)aromatic compounds are less soluble, often absorbed by soil organic matter (Borisover and Graber, 1997), but also more resistant against (bio)degradation (Ren et al., 2018). For all these compounds, sorption processes slow down their migration in environmental conditions (Curtis et al., 1986; Weber et al., 1991). Consequently, understanding retardation phenomena of soluble organic matter is crucial for bioavailability of solutes, remediation of soils, extraction of ore, or hazardous waste management. Several scientific communities have investigated such issues for specific media (soils, sand, sedimentary rocks, cement based materials...) or site specific conditions (acidic, neutral or alkaline, oxidant or reducing media...). For example, the migration of organic ligands was largely investigated in many oxide-rich soils and model materials (Liu et al., 2014). In this field, a good agreement is usually observed between adsorption measured by batch experiments, results from flow-through methods and field observations (Liu et al., 2013; Banzhaf and Hebig, 2016). Such approach requires determining and studying the relevant factors controlling site-specific transport, for example adsorption-dissociation processes (Zachara et al., 1995; Szecsody et al., 1998), slow kinetics-driven transport (Brusseau, 1991), colloidal effects (Roy and Dzombak, 1998), etc. Similar issue was recently raised for diffusion of organic anions in clay-rich rocks (Durge et al., 2014; Dagnelie et al., 2014).

In the past decade, a tremendous effort was made to study solutes migration phenomena in geological media in the context of deep underground radioactive wastes repository (Altman et al., 2012; Tournassat et al., 2015). Sedimentary clay rich rocks, such as the Callovo-Oxfordian mudstone (France), Boom clays (Belgium), Opalinus clays (Switzerland) were intensively studied in this context (Delage et al., 2010). They are characterized by low hydraulic conductivities and diffusion coefficients due to their narrow pore network and by high retention properties of cations due their affinity with the constituting clay minerals. In such rocks, the migration of cations is mainly driven by their adsorption on clay minerals (Melkior et al., 2007; Savoye et al., 2012; 2015). On the contrary, inorganic anions display a poor affinity for clay surfaces and they are repelled from the pore surface leading to the well-established “anion exclusion” phenomena (Bazer-Bachi et al., 2007; Descostes et al., 2008; Frasca et al., 2012; Montavon et al., 2014). The behaviour of small organic anions was found to be intermediate between those of cations and inorganic anions (Dagnelie et al., 2014). Small carboxylates are affected by “anion exclusion” as inorganic anions and displays retention properties as inorganic cations (Descostes et al., 2017). These compounds are studied for various safety assessments, including metal and radionuclides transport (Nowack et al., 1997; Read et al., 1998; Hummel, 2008; Charlet et al., 2017). Rasamimanana et al. (2017a) recently quantified and summarized the adsorption of various carboxylic anions (acetate, phthalate, citrate), deduced from batch experiments on Callovo-Oxfordian mudstone. Solid to liquid distribution coefficient (R_d) are ranged from 0.1 to several tens of $L.kg^{-1}$ demonstrating the significant affinity of the rock for these anions. Similar trends were recently confirmed by percolation experiments on compacted illite with hydrophilic hydroxyl-acids (Chen et al., 2018). Yet a key point remains unclear for organic anions, which is the discrepancy between high R_d values measured by batch experiments and low retardation factors measured by migration experiments (Dagnelie et al, 2014). The origin

of this discrepancy has to be cleared in order to predict the reactive transport of organics, as correctly achieved for other solutes.

The objective of this work was to evaluate the diffusive behaviour of various organic anions in a clay-rich sedimentary rock and compare diffusive retardation factors with adsorption data. This was performed in Callovo-Oxfordian clay rock, for which a clear picture of anion adsorption was available in the literature. A possible explanation is provided for the discrepancies previously observed between batch and diffusion experiments.

2. Material and methods

2.1 Rock samples

Experiments were carried out on samples originated from the Callovo-Oxfordian sedimentary formation (Meuse/Haute-Marne France). The rock cores, EST40471 and EST207_16517 and EST_16520, were drilled from a borehole in the underground laboratory at -501 m and -498 m in depth from the surface respectively. The claystone comes from the clayey unit constituted of clayey unit constituted by 50-55% of clay minerals (illite, interlayered illite-smectite, kaolinite, chlorite), 18 -20% of tectosilicates (mainly quartz), 22-35 % of carbonates (mainly calcite) and less than 5 % of accessory minerals (pyrite, iron oxide...). Organics matter is estimated to < 1% (COT ~ 0.6%) (Gaucher et al., 2004; Lerouge et al., 2011; Pellenard et al., 2014). The core sample was protected from O₂ after drilling using container under N_{2(g)}. Thanks to a wire saw inside a glovebox, the rock core were sliced into ~10 mm thick samples and then adjusted to 35 - 40 mm of diameter. The dimension of the samples is listed in supplementary data (Table S1). The weighting of solid samples led to an average hydrated density $\rho_H \sim 2.34 \pm 0.06 \text{ g cm}^{-3}$ leading to a total porosity of 21 % assuming a grain density, $\rho_g \sim 2.7 \text{ g cm}^{-3}$ ($\epsilon \sim [\rho_H - \rho_g] / [1 - \rho_g]$).

2.2 Diffusion experiments

Two main setups were used in this study and displayed a good repeatability (Table S1). The static setup includes a PEEK cell, a sample pasted with epoxy resin between two filterplates in contact with upstream / downstream solutions (see Descostes et al., 2008 for detailed setup). The dynamic setup includes a stainless steel cell, a sample swelled inside the cell without filterplates or resin, and in contact with solutions circulating in upstream / downstream reservoirs (see Savoye et al., 2011 for detailed setup). The list of diffusion experiments is detailed in Table 1, including each organic tracer monitored. Table 1 mostly gathers experimental results, including the diffusion data of organic tracers and when available, the diffusion data of inert tracers (HTO, HDO) used prior to experiments with organics. Complementary information is available in supplementary data (Table S1): size, activities, concentration, ionic strength. Experiments n°8 and 10 were performed in presence of competing solute, respectively $[\text{Na}_2\text{Phthalate}] = 10^{-1} \text{ M}$ and $[\text{NaISA}] = 10^{-2} \text{ M}$. The effect of these competing anions and of ionic strength will also be discussed furtherly.

2.3 Modelling

The solid to solution distribution ratio is noted R_d (L.kg^{-1}). It is defined and modelled by

$$R_d = \frac{C_{ads}}{C_e} \quad R_d(C_e) = \frac{K_L \times Q}{(1 + K_L \times C_e)} \quad (1)$$

where $C_{ads}(\text{mol kg}^{-1})$ is the concentration of adsorbed species per mass of adsorbent, and $C_e(\text{mol L}^{-1})$ the concentration in solution at equilibrium with the solid. The adsorption isotherms, $R_d(C_e)$, displayed a Langmuir-Type shape (Eq. 1) and parameters (K_L , Q) were quantified by Rasamimanana et al. (2017). The analysis of the through-diffusion results, which is based on Fick's second law:

$$\frac{\partial C}{\partial t} = \frac{D_e}{\varepsilon_a + \rho_g(1-\varepsilon)R_d^{APP}} \frac{\partial^2 C}{\partial x^2} = \frac{D_e}{\alpha} \frac{\partial^2 C}{\partial x^2} \quad (2)$$

with C representing the tracer concentration (mol m^{-3}), t the time (s), D_e the effective diffusion coefficient ($\text{m}^2 \text{s}^{-1}$), ε_a the diffusion-accessible porosity, ρ_g the grain density ($\sim 2.7 \text{ kg L}^{-1}$), R_d^{APP} the apparent adsorption coefficient, and α the rock capacity factor. $R = \alpha/\varepsilon_a$ is usually called the retardation factor. The initial conditions were $C(x=0) = C_0$, $C(x \neq 0) = 0$. Fully analytical solutions were performed to fit the results with a constant R_d^{APP} value. The resolution was performed by numerical resolution in the Laplace space (Crank, 1975; Moridis, 1998). The downstream flux of tracer, J ($\text{moles m}^{-2} \text{s}^{-1}$) was defined by equation (3):

$$J_{\text{down}}(t) = \frac{dn_{\text{down}}(t)}{S \times dt} = \frac{V_{\text{down}}}{S} \lim_{\Delta t \rightarrow 0} \frac{C_{\text{down}}(t + \Delta t) - C_{\text{down}}(t - \Delta t)}{2 \times \Delta t} \quad (3)$$

where dn_{down} is the quantity of tracer reaching the downstream compartment in (moles or Bq), per unit of time, dt (s), and sample surface S (m^2). V_{down} (m^3) is the downstream volume and Δt the duration between two successive measurements. In the case of experimental data, C_{down} (mol L^{-1}) was corrected from radioactive decay and sampling, and named cumulative concentration. All results are discussed on the basis of a normalised flux of tracer:

$$^{\text{NORM}}J_{\text{down}}(t) = \frac{L}{C_0} J_{\text{down}}(t) \quad (4)$$

with L (m) being the sample width and C_0 (moles m^{-3}) the initial concentration of tracer in upstream reservoir. By using $^{\text{NORM}}J_{\text{down}}$ ($\text{m}^2 \text{s}^{-1}$), the direct comparison of the different experiments was possible, regardless of C_0 or L . Experiments tend to move towards a stationary state where the flux is close to the effective diffusion coefficient $^{\text{NORM}}J_{\text{DOWN}}(t \rightarrow \infty) \sim D_e$, as long as upstream and downstream concentrations evolve slowly, $(C_{\text{up}} - C_{\text{down}})(t \rightarrow \infty) \sim C_0$.

The two parameters D_e and α were adjusted by least-square fitting of experimental normalized downstream flux with a weighting inversely proportional to the experimental

precision. The upstream concentration was not used at all for adjustment. This choice was made because specific effects (perturbation of speciation, non-reversible adsorption, slow kinetics) might lead to uncomplete mass balance between upstream and downstream measurements (Roberts et al., 1986). A good agreement between upstream experimental data and the modelling (adjusted on downstream data) only strengthens the reliability of the results. This was especially the case for exp. n°2, 3, 5, 7, 8, 12, 13, 14, 15.

3. Results

3.1 Diffusion of organic acids in Callovo-Oxfordian clay rock

A comparison between solutes is made in Figure 1 on the normalized fluxes and downstream cumulative concentration. For more details, the raw experimental data (downstream flux with precision, downstream cumulative concentration and upstream concentration) are given in supplementary data and compared with modelling (Fig. S1-S5). The normalized downstream fluxes (Fig. 1) rise to a plateau, which is representative of the effective diffusion coefficient of the solute, D_e . The corresponding values, $D_e^{ORGA} \sim 10^{-12} \text{ m}^2 \text{ s}^{-1}$ value (eq. 4), are much lower than effective diffusion coefficient of water ($D_e^{HTO} > 10^{-11} \text{ m}^2 \text{ s}^{-1}$). Similar behaviours were evidenced on inorganic anions in sedimentary rocks (Descostes et al., 2008; Van Loon and Mibus, 2015) as well as for organic acids in Callovo-Oxfordian clay rock (Dagnelie et al., 2014). The transitory state display various duration, from almost no retardation (for HTO, Acetate or Adipate), to a significant retardation observed for EDTA or Oxalate (up to 100 days).

The D_e and α values adjusted from experimental results (best fit) are gathered in Table 1. When available, the data of reference tracers (HDO, HTO), allow an estimation of variability from one sample to the other. A variability of a factor 3 is observed on diffusivities: D_e^{HTO} ranging from 1.5 to 4.5 $10^{-11} \text{ m}^2 \text{ s}^{-1}$. It is then much more reliable to

compare results normalized by the value of the reference tracer (HDO, HTO). This is performed by calculation of the factor Π given by the following equation:

$$\Pi = \frac{[D_e^{ANION}/D_0^{ANION}]}{[D_e^{REF}/D_0^{REF}]} \quad (5)$$

Where D_e is the effective diffusion coefficient in the porous solid and D_0 the diffusion coefficient in water. D_0 values are corrected from the effect of salinity (I.S. ~ 0.105 eq. in Callovo-Oxfordian porewater and from Temperature, $T^{EXP.} \sim 22 \pm 2$ °C). Superscripts refer to the solutes, which are either anions (Cl^- , Organic) or neutral references (HTO or HDO). The ratio: Π isolates the effect of clay on the diffusion pathway of anions (i.e. tortuosity and constrictivity as discussed by Van Brakel and Heertjes, 1974). For example, a reduced accessible porosity for anions, ϵ_a , induces a lower diffusivity than that of water, $\Pi < 1$. Several empirical observations evidenced this correlation between Π measured in sedimentary rocks and ϵ_a/ϵ , which is a quantification of the anion exclusion. The most common model is the empirical Archie's law (Eq. (6), Archie (1942), with $m \sim 2.4$), and further adaptations in various media, such as m-Archie's law (Eq. (7), Jacquier et al. (2013) with $\alpha = 0.17$ and $m = 1.6$) developed for Callovo-Oxfordian clay samples of variable mineralogy, or also e-Archie's law (Eq. (8), Van Loon et al. (2015), with $B=10^{-11} \text{ m}^2 \text{ s}^{-1}$, $m_1 = 2.4$ and $m_2 = 1$) adjusted on low porosity materials ($\epsilon < 2 \cdot 10^{-2}$).

$$\frac{D_e}{D_0} = \epsilon^m \quad (6)$$

$$\frac{D_e}{D_0} = \alpha \times \epsilon^m \quad (7)$$

$$D_e = D_0 \times \epsilon^{m_1} + B \times \epsilon^{m_2} \quad (8)$$

3.2 Effect of Ionic Strength and anion exclusion

Two important features arise from the previous results. First, the low Π ratios for organic anions in Callovo-Oxfordian clay rock, $0.1 < \Pi < 0.5$, traduce a strong but variable exclusion for these compounds probably originating from charge and or steric effects. Nevertheless, adsorption occurs for these compounds, and the apparent porosity $\alpha(\text{orga})$ differs from accessible porosity $\epsilon_a(\text{orga})$, which remains hardly measurable by direct methods. Thus the parameter Π seems the most reliable and accurate data to quantify an accessible porosity for organic anions: $\epsilon_a(\text{orga})$. Still, this requires to choose carefully one of the above the empirical laws, i.e. the most suitable for the studied material.

The figure 2 illustrates the diffusivity of chloride, taken as a non sorbing anion in clay-rich media. It was measured by through-diffusion through Callovo-Oxfordian samples (Blin et al., 2013) and percolation through compacted illite samples (Chen et al., 2018). The variability was induced by experimental setup, performed several times under various ionic strengths. The increase of ionic strength is known to reduce the size of the diffuse layer at the surface of charged minerals, thus decreasing anion exclusion. This is indeed observed on both D_e and ϵ_a values and allows a verification of Archie's law as performed in Fig. 2. A comparison is made with other data from literature on clay rich media (various contents of illite, smectite and kaolinite minerals). It ensures that the correlation $\Pi = f(\epsilon_a/\epsilon)$ follows similar trends for all the discussed media. This legitimates further comparison of these systems and the use of m-Archie law following Eq. (7) (Jacquier et al., 2013) for these results. This law was used to calculate the ϵ_a/ϵ values for organic solutes, and data are reported in both table 1 and Figure 3.

3.2 Variability of retardation factor

Only a few studies assess the effect of porosity exclusion on retardation factors in clay-rich media. Usually in such media, the Eq. (2) is admitted assuming the following hypotheses: i) Adsorption only occurs for cations for which all the porosity is accessible, i.e. $\varepsilon(\text{cations}) = \varepsilon$, ii) Anions, for which $\varepsilon_a(\text{anions}) < \varepsilon$, display a negligible adsorption i.e. $R_d^{APP} = 0$. This is true for most of the inorganic anions in Callovo-Oxfordian clay rock, but is not true for oxoanions or organic anions (Frasca et al., 2014; Rasamimanana et al., 2017). Indeed, the organic anions display both properties of adsorption ($R_d^{APP} > 0$) and of anion exclusion $\varepsilon_a(\text{orga}) < \varepsilon$. This latter property possibly induces a modification of the retardation factor. The exclusion of solutes from a part of porosity may reduce the accessibility to surfaces and eventually lengthen the diffusion pathway (tortuosity). Such effect would decrease the apparent adsorption R_d^{APP} during transport. A similar effect was demonstrated by diffusion of solutes in unsaturated samples by Savoye et al. (2012c and 2017). The authors showed that the decrease of water-filled porosity was leading to a decrease of Cesium diffusivity and adsorption. To quantify such effects on organic anions, we gathered results performed at various ionic strengths with ^{14}C -oxalate and other small carboxylates (data from Chen et al., 2018). In this latter case, the R_d^{MAX} values were calculated by extrapolation of percolation results at infinite ionic strength (Fig. S6, table S3). The Fig. 2 illustrates the correlation between anion exclusion ($\varepsilon_a/\varepsilon$) and adsorption during transport (R_d/R_d^{MAX}). A trend is observed and could be adjusted by an exponential law of the following form:

$$\frac{R_d^{APP}}{R_d^{MAX}} = f^{CORR} = \frac{1}{\left[1 + \exp\left(a \times \left(b - \frac{\varepsilon_a}{\varepsilon}\right)\right)\right]} \quad (9)$$

This empirical law traduces a decrease of R_d^{APP} with exclusion ($\varepsilon_a/\varepsilon < 1$). The law starts from a maximum value, $R_d^{APP} = R_d^{MAX}$, in absence of exclusion ($\varepsilon_a = \varepsilon$, all surfaces accessible). A threshold appears at a value $\varepsilon_a/\varepsilon = b$, with a collapse of R_d^{APP} when $\varepsilon_a/\varepsilon < b$. In our case, the best fit parameters were $a = 12.95$ and $b = 0.60$. This adjustment remains empirical and such

law should be studied in detail for each porous media. However, such behaviour shows potential implications which are discussed furtherly. To that aim, the Eq. (7) provides a correction factor, f^{CORR} , leading to a generalized diffusion law:

$$\frac{\partial C}{\partial t} = \frac{D_e}{\alpha} \frac{\partial^2 C}{\partial x^2} = \frac{D_e}{\varepsilon_a + \rho_g(1-\varepsilon)f^{CORR}R_d^{CELL}} \frac{\partial^2 C}{\partial x^2} \quad (10)$$

4. Discussion

The following discussion assesses the generalized law, Eq. (10), by comparison between data from batch and diffusion experiments. The validity of such approach is discussed with emphasis on retardation variability and environmental implications.

4.1 Comparison between batch and diffusion experiments

The table 1 gathers adsorption data on 15 diffusion experiments, using 8 different organic anions of various polarities. Batch data were compare to diffusion data, using the following equations:

$$R_d^{BATCH} = \frac{1}{L} \int_{x=0}^L R_d\left(\frac{C_0 x}{L}\right) dx = \frac{Q}{C_0} \times \ln(1 + K_L \times C_0) \quad (11)$$

$$R_d^{APP} = \frac{(\alpha - \varepsilon_a)}{\rho_g(1-\varepsilon)} \quad R_d^{CELL} = \frac{(\alpha - \varepsilon_a)}{\rho_g(1-\varepsilon)f^{CORR}\left(\frac{\varepsilon_a}{\varepsilon}\right)} \quad (12)$$

The Eq. (11) traduces the adsorption expected in diffusion experiment, calculated thanks to batch data. A linear concentration profile along the diffusion cell is assumed, $C(x) = C_0 \times [x/L]$, and averaged using the Langmuir law, defined in Eq.1: $R_d(C) = f(Q, K_L, C)$.

The Eq. (12) traduces the adsorption directly extrapolated from diffusion data, using the adjusted apparent porosity, α , with (eq. 2) or without (eq. 10) the correction factor defined above.

The Figure 4 illustrates the comparison between batch and diffusion data. The red triangles show R_d^{APP} as a function of R_d^{BATCH} . Using raw batch data may lead to a significant overestimation of apparent porosity and retardation factor. The green triangles show R_d^{CELL} as a function of R_d^{BATCH} . A fairly good agreement is observed between batch data and diffusion data corrected from exclusion effects. The proposed correction factor is only a rough empirical adjustment, and no tool for accurate prediction of retardation factors. However, it strengthens the hypothesis of porosity exclusion as the key parameter affecting diffusive retardation. This feature would explain various effects observed on several species. For example, ionic strength effects are observed in the case of oxalate with the decrease of α and R_d^{APP} by a factor 2 when ionic strength increases between Exp. n°7 and 8. Also a large difference of retardation was observed between Eu-EDTA and EDTA species. This would be explained by a higher exclusion of the latter, as quantified by D_e values. This specific case leads to the following discussion on the origin of exclusion.

4.2 Origin of exclusion from the porosity

An interesting feature is the origin of the exclusion of adsorbates. Two specific effects are viewed in this study: i.e. steric and charge effects. It seems clear that formal charge is not a good indicator of electrostatic effects, as observed with inorganic anions (Descostes et al., 2008; Wigger and Van Loon, 2017). Still, charge effects are expected in clay rich media, and most probably linked to charge density, polarizability, or even hardness of anionic Lewis bases. Such assumption can be made in view of experimental results. For example, the diffusion of small anion NO_3^- in Callovo-Oxfordian clay rock, displayed a much lower exclusion than for Cl^- , $\Pi(NO_3^-) \sim 0.7 \gg \Pi(Cl^-) \sim 0.4$ (Dagnelie et al., 2017). This result agrees with a lower exclusion of NO_3^- , of which charge is distributed between 3 atoms compared to Cl^- . In the present study also, the values $\Pi(oxalate) \sim 0.25-0.36$ were lower than

Π (o-phthalate)~0.1-0.25, despite a larger size for the latter. This also indicates possible charge effects in addition to steric effects. Yet, it is not clear for organic anions, which parts of exclusion are due to charge effect and steric effect. In addition to charge exclusion, larger molecule may be more excluded from porosity, due to the presence of small porosity in clay rich media (Gaboreau et al., 2016; Wigger and Van Loon, 2018). Such hypothesis seems confirmed by the correlation between Π and molecule size (Fig. S7). Obviously, such relationship remains a trend rather than a well-defined correlation, given that two factors are simultaneously involved, i.e. charge and size. Further studies would be interesting to decorrelate both effects using molecules of well-known properties. To that aim, D_e and Π values should be measured more accurately and preferentially on the same sample. Also molecular size should take into account speciation in solution and hydration shell of species. Finally, additional modelling seem mandatory to quantify relevant electric properties of adsorbates (charge density, shape and energy of the highest occupied molecular orbital, etc.).

4.3 Methodology and environmental implications

The easiest method to quantify adsorption involves usually batch experiments on crushed samples. Such approach is commonly preferred to diffusion experiments, much more time consuming, or percolation experiments involving other processes and possible bias (advection, dispersion, minerals leaching). The previous findings highlight the difficulty to predict retardation factors in clay-rich media only based on adsorption data, especially for organic anions. A generalized law is proposed for adsorption-diffusion with equation (10). It is in agreement with classical laws for cations and non-sorbing anions. In the case of adsorbing anions, it includes an additional effect due to porosity exclusion. This effect should be studied first, in order to assess the shape of $f^{CORR}(\epsilon_a/\epsilon)$ curve. This empirical factor does not exempt from performing diffusion experiments, as they provide the most accurate

estimation α parameter. In addition, the quantification of D_e/D_0 also seems mandatory to get an estimation of the exclusion of sorbing anions, ϵ_a/ϵ . To that aim, the use of an inert tracer (HTO, HDO) as reference is highly recommended, since D_e values display a variability of a factor 2 to 3 among similar samples. Also the extrapolation of ϵ_a/ϵ using D_e/D_0 value requires the choice an Archie's-type law suitable for the material.

In the case of clay rocks, a low diffusivity for organic anions is evidenced with D_e values ranging between 0.8 and $7 \cdot 10^{-12} \text{ m}^2 \text{ s}^{-1}$. The adsorption properties might lead to high apparent porosity as observed for oxalate or ISA. However, the species with lowest diffusivities, $D_e < 2 \cdot 10^{-12} \text{ m}^2 \text{ s}^{-1}$ may present an important anion exclusion leading to a strongly reduced retardation. Similar methodologies should be suitable in other material but taking account of the media specificity. Depending on the materials, sorbing or non-sorbing species differs leading to various reference solutes (Schaffer et al., 2017). It would be interesting to perform such comparative studies on various media such as oxisoils, sediments or cementitious materials.

5. Conclusions

In this study we evaluated diffusive data of eight organic anions through Callovo-Oxfordian clay rock, a clay-rich sedimentary rock. The affinities of organic anions for rock surfaces induced various retardation factors. However, a significant discrepancy was observed between maximum adsorption data measured by batch experiments and apparent adsorption extrapolated from diffusive retardation. A qualitative explanation is proposed based on porosity exclusion, probably due to both steric and charge effects. The decrease of accessible porosity for a solute may modify accessible surface or tortuosity, thus leading to a reduced retardation. This was observed on both compacted clay minerals and Callovo-Oxfordian clay rock. A threshold value of ϵ_a/ϵ is eventually observed under which the retardation of sorbing

species collapses. This feature should be assessed and valuate for each specific solute/media couple. This may be achieved in the case sorbing anions in clay-rich media, using various ionic strengths, which impact both accessible porosity and retardation factor.

In a first approximation, an empirical correction factor $[1/(1+a \times \exp(b - \epsilon_a/\epsilon))]$ was proposed. This factor estimates the ratio between apparent and maximum adsorption during migration in a porous media. It was evaluated for Callovo-Oxfordian clay rock thanks to diffusion data and percolation through compacted illite. The parameters $a = 12.95$ and $b = 0.60$ were adjusted and used to estimate adsorption from 15 diffusion experiments. A reasonable agreement was observed between adsorption experiments in batches and diffusion experiments in cell. The low diffusivity of organic species is confirmed, with D_e values ranging between 0.5 and $7 \cdot 10^{-12} \text{ m}^2 \text{ s}^{-1}$. These values traduce anion exclusion from porosity probably due to charge and possibly with additional steric effects. The effective diffusion was necessary to evaluate the accessible porosity (anion exclusion), following m-Archie law. Finally, a significant retardation was observed for several species, such as oxalate of ISA. Still, this retardation factor strongly decreased for the most excluded species, i.e. with values $\epsilon_a/\epsilon \ll b = 0.60$, or $D_e < 2 \cdot 10^{-12} \text{ m}^2 \text{ s}^{-1}$.

The proposed methodology should be applicable to other media with charged surfaces such as cementitious materials or oxisoils. It would be interesting to compare such results, since the solutes affinity or exclusion will differ from one media to the other. Such approach could help assessing the transport of organic solutes in the environment.

Acknowledgments

In memory of Dr. Eric Giffaut. This work was partially financed by the National Radioactive Waste Management Agency (Andra). We thank F. Goutelard for early diffusive experiments at

various ionic strength. We gratefully thank two anonymous reviewers for their constructive comments and suggestions.

References

Archie, G.E., 1942. The electrical resistivity log as an aid in determining some reservoir characteristics. *Trans. AIME* 146, 54–62.

Banzhaf, S., Hebig, K., 2016. Use of column experiments to investigate the fate of organic micropollutants - a review. *Hydrol. Earth Syst. Sci.*, 20, 3719–3737.

Bazer-Bachi, F., Descostes, M., Tevissen, E., Meier, P., Grenut, B., Simonnot, M.-O. Sardin, M. 2007. Characterization of sulphate sorption on Callovo-Oxfordian argillites by batch, column and through-diffusion experiments, *Physics and Chemistry of the Earth, Parts A/B/C*, 32, 8–14.

Blin, V., Arnoux, P., Hainos, D., Radwan, J., 2013. Influence of a saline plume (NaNO₃) on radionuclide mobility in the Callovo-Oxfordian clay rock. *Radionuclide Migration Conference*, 2013 09 08-13, Brighton, UK.

Borisover, M., Graber, E.R., 1997. Specific interaction of Organic compounds with soil organic carbon. *Chemosphere* 34, 8, 1761-1776.

Borisover, M., Davis, J., 2015. Adsorption of inorganic and organic solutes by clay minerals. in: Tournassat, C., Steefel, C., Bourg, I.C., Bergaya, F. (Eds.), *Natural and Engineered Clay Barriers*. Elsevier.

Brusseau, M.,L., 1991. Nonequilibrium Sorption of Organic Chemicals: Elucidation of Rate-Limiting Processes. *Environ. Sci. Technol.* 25, 134-142.

Charlet, L., Alt-Epping, P., Wersin, P., Gilbert, B., 2017. Diffusive transport and reaction in clay rocks: A storage (nuclear waste, CO₂, H₂), energy (shale gas) and water quality issue. *Adv. Water Res.* 106, 39-59.

403 Chen, Y., Glaus, M.A., Van Loon, L.R., Mäder, U. 2018. Transport of low molecular weight
404 organic compounds in compacted illite and kaolinite. *Chemosphere* 198, 226-237.

405 Curtis, G.P., Roberts, P.V., Reinhard, M. 1986. A Natural Gradient Experiment on Solute
406 Transport in a Sand Aquifer 4. Sorption of Organic Solutes and its Influence on Mobility.
407 *Wat. Res. Research* 22, 13, 2059-2067.

408 Crank, J., 1975. *The Mathematics of Diffusion*. Clarendon Press, London.

409 Dagnelie, R.V.H., Arnoux, P., Radwan, J., Lebeau, D., Nerfie, P., Beaucaire, C., 2015.
410 Perturbation induced by EDTA on HDO, Br⁻ and Eu^{III} diffusion in a large-scale clay rock
411 sample. *Appl. Clay Sci.* 105-106, 142–149.

412 Dagnelie, R.V.H., Descostes, M., Pointeau, I., Klein, J., Grenut, B., Radwan, J., Lebeau, D.,
413 Georgin, D., Giffaut, E., 2014. Sorption and diffusion of organic acids through clayrock:
414 comparison with inorganic anions. *J. Hydrol.* 511, 619-627.

415 Dagnelie, R.V.H., Rasamimanana, S., Thory, E., Lefèvre, G., 2017. Competitive adsorption of
416 organic molecules on sediments. *Procedia Earth Plan. Sci.* 17, 144-147.

417 Delage, P., Cui., Y.J., Tang, M., 2010. Clays in radioactive waste disposal. *J. Rock. Mech.*
418 *And Geotech. Eng.* 2 (2), 111-123.

419 Descostes, M., Blin, V., Bazer-Bachi, F., Meier, P., Grenut, B., Radwan, J., Schlegel, M.L.,
420 Buschaert, S., Coelho, D., Tevissen, E., 2008. Diffusion of anionic species in Callovo-
421 Oxfordian argillites and oxfordian limestones (Meuse/Haute-Marne, France). *Appl. Geochem.*
422 23, 655–677.

423 Descostes, M., Pointeau, I., Radwan, J., Poonosamy, J., Lacour, J.-L., Menut, D., Vercouter,
424 T., Dagnelie, R.V.H. , 2017. Adsorption and retarded diffusion of Eu^{III}-EDTA⁻ through hard
425 clay rock. *J. Hydrol.* 544,125-132.

426 Duarte, R., Matos, J., Senesi, N., 2018. Chapter 5 - Organic Pollutants in Soils, In *Soil*
427 *Pollution*, edited by A. C. Duarte, A. Cachada and T. Rocha-Santos, Academic Press, 103–

428 126.

429 Durce, D., Landesman, C., Grambow, B., Ribet, S., Giffaut, E., 2014. Adsorption and
430 transport of polymaleic acid on Callovo-Oxfordian clay stone: batch and transport
431 experiments. *J. Contam. Hydrol.* 164, 308-322.

432 Frasca, B., Savoye, S., Wittebroodt, C., Leupin, O.X., Descostes, M., grenut, B., Etep-
433 Batanken, J., Michelot, J-L., 2012. Influence of redox conditions on iodide migration
434 through a deep clay formation (Toarcian argillaceous rock, Tournemire, France). *Appl.*
435 *Geochem.* 27, 2456-2462.

436 Frasca, B., Savoye, S., Wittebroodt, C., Leupin, O.X., Michelot, J.-L., 2014. Comparative
437 study of Se oxyanions retention on three argillaceous rocks: Upper Toarcian (Tournemire,
438 France), Black Shales (Tournemire, France) and Opalinus Clay (Mont Terri, Switzerland). *J.*
439 *Environ. Rad.* 127, 133-140.

440 Gaboreau, S., Robinet, J.-C., Prêt, D., 2016. Optimization of pore-network characterization of
441 a compacted clay material by TEM and FIB/SEM imaging. *Microp. Mesopo. Materials* 224,
442 116-128.

443 Gaucher, E., Robelin, C., Matray, J., Negrel, G., Gros, Y., Heitz, J., Vinsot, A., Rebours, H.,
444 Cassagnabère, A., Bouchet, A., 2004. ANDRA underground research laboratory:
445 interpretation of the mineralogical and geochemical data acquired in the Callovo-Oxfordian
446 formation by investigative drilling. *Phys. Chem. Earth* 29, 55-77.

447 Hummel, W., 2008. Radioactive contaminants in the subsurface: the influence of complexing
448 ligands on trace metal speciation. *Monatshefte für Chemie – Chem. Mon.* 139, 459–480.

449 Jacquier, P., Hainos, D., Robinet, J.-C., Herbette, M., Grenut, B., Bouchet, A., Ferry, C.,
450 2013. The influence of mineral variability of Callovo-Oxfordian clay rocks on radionuclide
451 transfer properties. *Applied Clay Sci.* 83-84, 129-136.

452 Keith-roach, M.J., 2008. The speciation, stability, solubility and biodegradation of organic co-
 453 contaminant radionuclide complexes: A review. *Sci. Total Environ.* 96, 1–11.

454 Keller, A.A., Wang, H., Zhou, D., Lenihan, H.S., Cherr, G., Cardinale, B.J., Miller, R., Ji, Z.,
 455 2010. Stability and Aggregation of Metal Oxide Nanoparticles in Natural Aqueous Matrices
 456 *Environ. Sci. Technol.* 44 (6), 1962–1967.

457 Lerouge, C., Grangeon, S., Gaucher, E.C., Tournassat, C., Agrinier, P., Guerrot, C. Widory,
 458 D., Fléhoc, C., Wille, G., Ramboz, C., Vinsot, A., Buschaert, S., 2011. Mineralogical and
 459 isotopic record of biotic and abiotic diagenesis of the Callovo-Oxfordian clayey formation of
 460 Bure (France). *Geochim. Cosmochim. Acta* 75 (10), 2633-2663.

461 Liu, H., Chen, T., Frost, R.L., 2014. An overview of the role of goethite surfaces in the
 462 environment. *Chemosphere* 103, 1-11.

463 Melkior, T., Yahiaoui, S., Thoby, D., Motellier, S., Barthes, V., 2007. Diffusion coefficients
 464 of alkaline cations in Bure mudrock. *Phys. Chem. Earth Parts A/B/C* 32, 453–462.

465 Montavon, G., Sabatié-Gogova, A., Ribet, S., Bailly, C., Bessaguet, N., Durce, D., Giffaut, E.,
 466 Landesman, C., Grambow, B., 2014. Retention of iodide by the Callovo-Oxfordian formation:
 467 An experimental study. *Appl. Clay Sci.* 87, 142–149.

468 Moridis, G.J., 1998. A Set of semianalytical solutions for parameter estimation in diffusion
 469 cell experiments. *Sci. York*.

470 Nowack, B., Xue, H., Sigg, L. 1997. Influence of Natural and Anthropogenic Ligands on
 471 Metal Transport during Infiltration of River Water to Groundwater. *Environ. Sci. Technol.* 31,
 472 866-872.

473 Pellenard, P., Deconinck, J.-F., 2014. Mineralogical variability of callovo-oxfordian clays
 474 from the paris basin and the subalpine basin. *C.R. Geosci.* 338, 854-866.

475 Rasamimanana, S. Rétention et transport diffusif d'anions organiques dans la roche argileuse
 476 du Callovo-Oxfordien ; Ph.D. Thesis, Université Pierre et Marie Curie Paris-VI, France, 2016.

477 Rasamimanana, S., Lefèvre, G., Dagnelie, R., 2017. Various causes behind desorption
478 hysteresis of carboxylic acids on mudstones. *Chemosphere* 168, 559-567.

479 Read, D., Ross, D., Sims, R.J. 1998. The migration of uranium through Clashach Sandstone:
480 the role of low molecular weight organics in enhancing radionuclide transport. *J. Contam.*
481 *Hydrol.* 35, 235-248.

482 Ren, X., Zeng, G., Tang, L., Wang, J., Wan, J., Liu, Y., Yu, J., Yi, H., Ye, S., Deng, R., 2018.
483 Sorption, transport and biodegradation – An insight into bioavailability of persistent organic
484 pollutants in soil. *Sci. Total Environ.* 610–611, 1154-1163.

485 Roberts, P.V., Goltz, M.N., Mackay, D.M. 1986. A Natural Gradient Experiment on Solute
486 Transport in a Sand Aquifer 3. Retardation Estimates and Mass Balances for Organic Solutes.
487 *Wat. Res. Research* 22, 13, 2047-2058.

488 Roy, S.B., Dzombak, D.A. 1998. Sorption nonequilibrium effects on colloid-enhanced
489 transport of hydrophobic organic compounds in porous media. *J. Contam. Hydrol.* 30, 179-
490 200.

491 Savoye, S., Goutelard, F., Beaucaire, C., Charles, Y., Fayette, A., Herbette, M., Larabi, Y.,
492 Coelho, D., 2011. Effect of temperature on the containment properties of argillaceous rocks:
493 The case study of Callovo–Oxfordian claystones. *J. Contam. Hydrol.* 125, 102-112.

494 Savoye, S., Beaucaire, C., Fayette, A., Herbette, M., Coelho, D., 2012a. Mobility of cesium
495 through the Callovo-Oxfordian claystones under partially saturated conditions. *Environ. Sci.*
496 *Technol.* 46, 2633–2641.

497 Savoye, S., Frasca, B., Grenut, B., Fayette, A., 2012b. How mobile is iodide in the Callovo–
498 Oxfordian claystones under experimental conditions close to the in situ ones?, *J. Contam.*
499 *Hydrol.* 142–143, 82-92.

500 Savoye, S., Beaucaire, C., Fayette, A., Herbette, M., Coelho, D., 2012c. Mobility of Cesium
501 through the Callovo-Oxfordian Claystones under Partially Saturated Conditions. *Envir. Sci.*

502 Tech. 46, 2633-2641.

503 Savoye, S., Beaucaire, C., Grenut, B., Fayette, A., 2015. Impact of the solution ionic strength
504 on strontium diffusion through the Callovo-Oxfordian clayrocks: an experimental and
505 modelling study. *Appl. Geochem.* 61, 41–52.

506 Savoye, S., Lefèvre, S., Fayette, A., Robinet, J.-C., 2017. Effect of Water Saturation on the
507 Diffusion/Adsorption of ^{22}Na and Cesium onto the Callovo-Oxfordian Claystones. *Geofluids*.
508 1683979, 17p.

509 Schaffer, M., Licha, T., 2015. A framework for assessing the retardation of molecules in
510 groundwater: Implications of the species distribution for the sorption-influenced transport.
511 *Sci. Total Environ.* 524-525, 187-194.

512 Schaffer, M., Warner, W., Kutzner, S., Börnick, H., Worch, E., Licha, T., 2017. Organic
513 molecules as sorbing tracers for the assessment of surface areas in consolidated aquifer
514 systems. *J. Hydrology*, 546, 370-379.

515 Szecsody, J.E., Zachara, J.M., Chilakapati, A., Jardine, P.M., Ferreny, A.S., 1998.
516 Importance of flow and particle-scale heterogeneity on $\text{Co}^{\text{II/III}}$ EDTA reactive transport. *J.*
517 *Hydrol.* 209, 112–136.

518 Tournassat, C., Steefel, C. I., Bourg, I. C., Bergaya, F. Editor(s), *Natural and Engineered Clay*
519 *Barriers*, In *Developments in Clay Science*, Elsevier, 2015. 6, 1572-4352.

520 Van Loon, L.R., Mibus, J., 2015. A modified version of Archie’s law to estimate effective
521 diffusion coefficients of radionuclides in argillaceous rocks and its application in safety
522 analysis studies. *Applied Geochem.* 59, 85-94.

523 Vinsot, A., Anthony, C., Appelo, J., Lundy, M., Wechner, S., Cailteau-Fischbach, C., de
524 Donato, P., Pironon, J., Lettry, Y., Lerouge, C., De Cannière, P., 2017. Natural gas extraction
525 and artificial gas injection experiments in Opalinus Clay, Mont Terri rock laboratory
526 (Switzerland). *Swiss J. Geosci.* 110, 375-390.

527 Weber, W.J.Jr., McGinley, P.M., Katz, L.E. 1991. Sorption phenomena in subsurface
528 systems: concepts, models and effects on contaminant fate and transport. *Wat. Res.* 25, 5,
529 499-528.

530 Wigger, C., Gimmi, T., Muller, A., Van Loon, L.R., 2018. The influence of small pores on the
531 anion transport properties of natural argillaceous rocks – A pore size distribution investigation
532 of Opalinus Clay and Helvetic Marl. *Applied Clay Sci.* 156, 134-143.

533 Wigger, C., Van Loon, L.R., 2017. Importance of interlayer equivalent pores for anion
534 diffusion in clay-rich sedimentary rocks. *Environ. Sci. Technol.* 51 (4), 1998–2006.

535 Zachara, J.M., Gassman, P.L., Smith, S.C., Taylor, D., 1995. Oxidation and adsorption
536 of Co(II) EDTA²⁻ complexes in subsurface materials with iron and manganese oxide grain
537 coatings. *Geochim. Cosmochim. Acta* 59, 4449–4463.

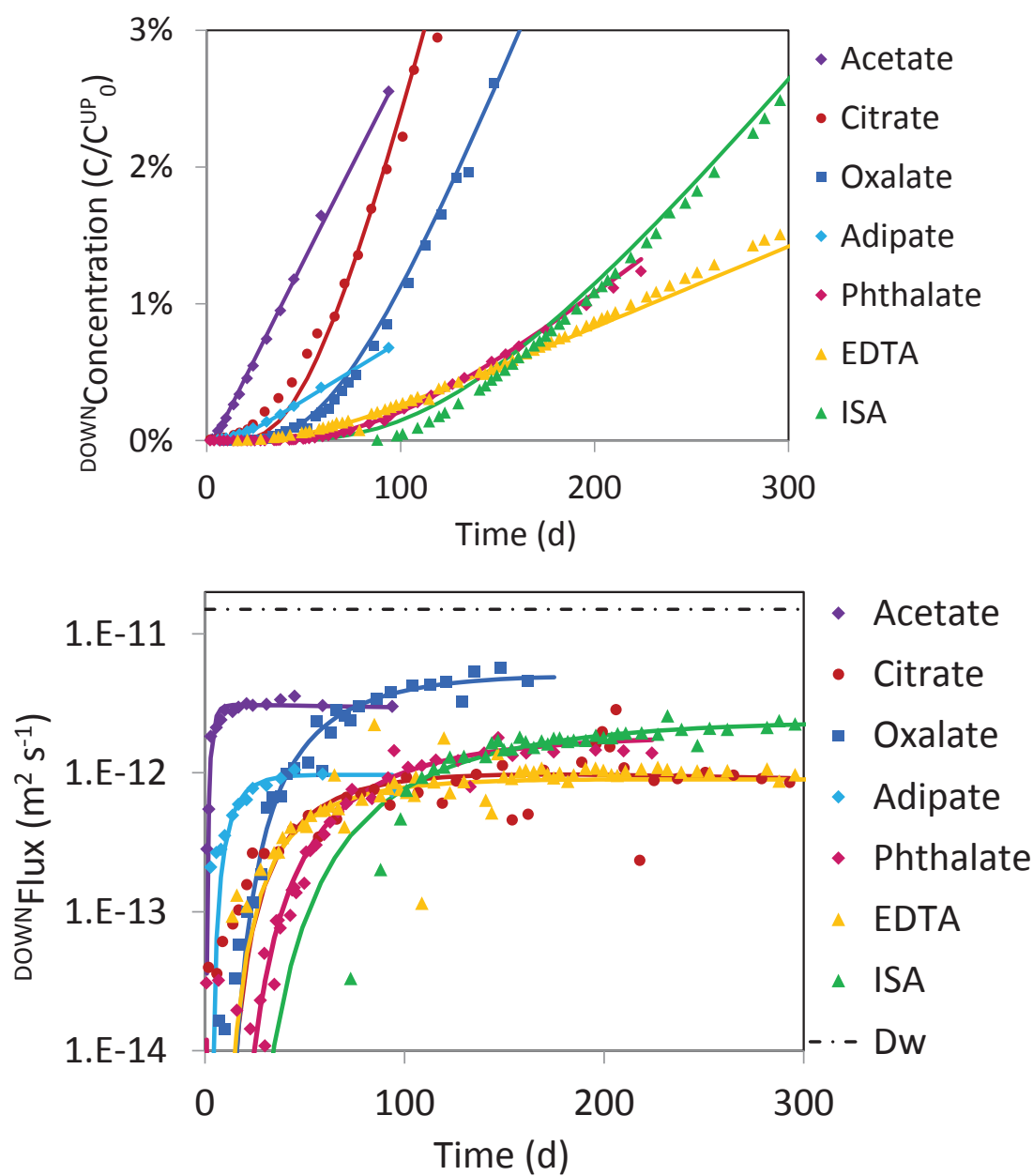


Figure 1: Illustration of diffusion experimental results.

Signs represent experimental data and solid curve represent best fit modelling. (Top) Downstream concentration as a function of time. Values normalized by initial upstream concentration.

(Bottom) Normalized downstream flux used for parametric adjustment.

D_w indicates the minimum D_e value measured for water: $D_e^{\text{MIN}}(\text{HTO}) = 15 \cdot 10^{-11} \text{ m}^2 \text{ s}^{-1}$.

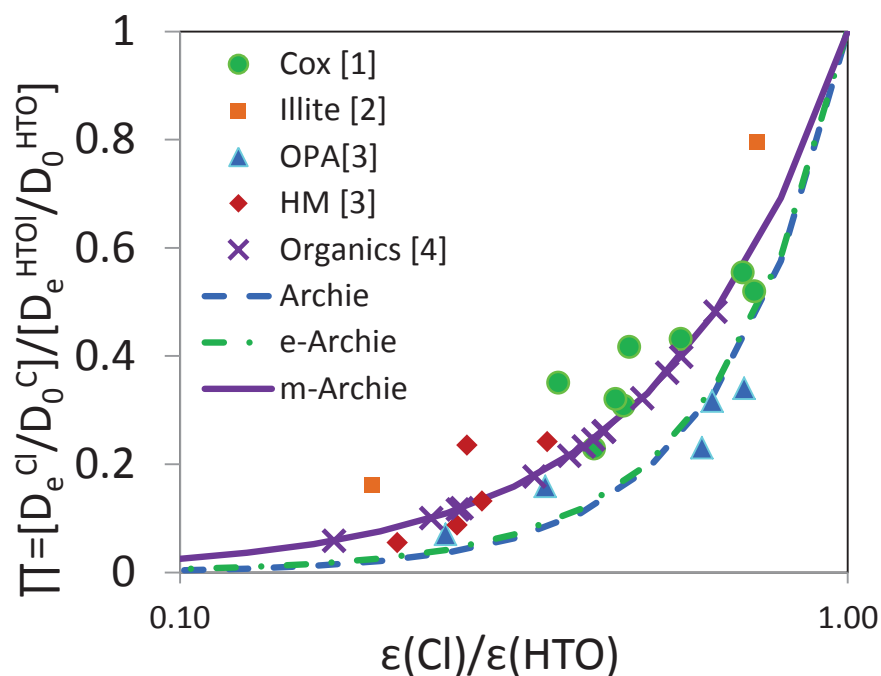


Figure 2: Effect of anion exclusion on diffusion parameters of chloride (Cl⁻). [1] Cl diffusion in COx at various Ionic strengths. (Unpublished, CEA/Andra, internal report) [2] Percolation experiments in compacted illite (Chen et al., 2018). [3] Diffusion experiments in Opalnius Clay (OPA) and Helvetic Marl (HM) (Wigger and van Loon, 2017). [4] Crosses represent Π values of organics measured in this study. Values were used to extrapolate ϵ_a/ϵ according to an m-Archie law (Jacquier et al., 2013).

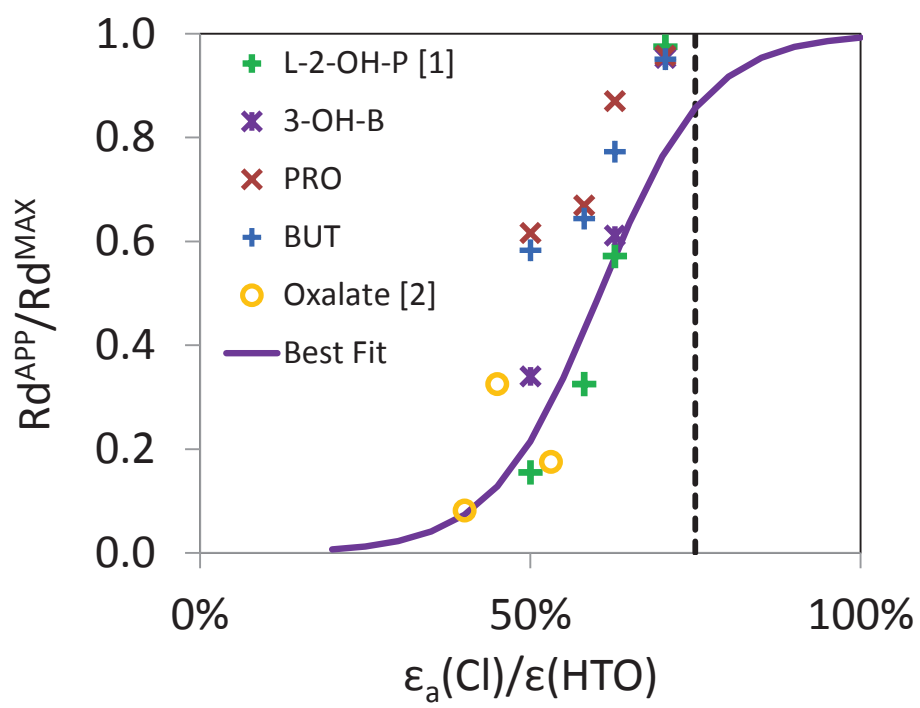


Figure 3: Effect of anion exclusion on adsorption of carboxylic acids in clay rich media.

[1] Percolation in compacted illite (Chen et al., 2018; R_d^{MAX} extrapolated at high ionic strength).

[2] Diffusion in Callovo-Oxfordian clay rock (This study, R_d^{MAX} measured by batch experiments).

Solid curve, best fit performed with all experimental data.

Dashed line represents the maximum ϵ_a/ϵ values reached at high ionic strength.

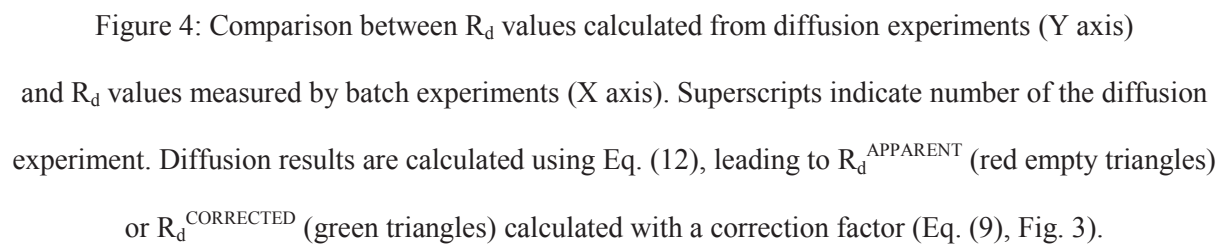


Figure 4: Comparison between R_d values calculated from diffusion experiments (Y axis) and R_d values measured by batch experiments (X axis). Superscripts indicate number of the diffusion experiment. Diffusion results are calculated using Eq. (12), leading to R_d^{APPARENT} (red empty triangles) or $R_d^{\text{CORRECTED}}$ (green triangles) calculated with a correction factor (Eq. (9), Fig. 3).

Table 1. Diffusion parameters adjusted from experiments. Taken from [a] Dagnelie et al., 2014 [b] Descostes et al., 2017, [c] this work.

Data in italic were not available and taken from average on similar samples. Data in bold are calculated using eq. 6, 7, 9 & 10.

n°/ref	Tracer	D_e^{HTO} (m ² s ⁻¹)	ε^{HTO} (%)	D_e^{ORGA} (m ² s ⁻¹)	α^{ORGA} (°)	Π^{ORGA}	ε_a^{ORGA} (°)	R_d^{APP} (L kg ⁻¹)	R_d^{CELL} (L kg ⁻¹)	R_d^{BATCH} (L kg ⁻¹)
1 [a]	¹⁴ C-EDTA	<i>3.60E-11</i>	<i>18.0%</i>	8.90E-13	0.25	1.16E-01	0.047	0.1	6.5	8.3
2 [a]	¹⁴ C- α -ISA	<i>3.60E-11</i>	<i>18.0%</i>	2.97E-12	2.60	2.33E-01	0.072	1.1	15.1	13.2
3 [a]	¹⁴ C-Phthalate	<i>3.60E-11</i>	<i>18.0%</i>	2.50E-12	0.86	2.46E-01	0.075	0.4	4.0	1.4
4 [a]	¹⁴ C-Oxalate	<i>3.60E-11</i>	<i>18.0%</i>	3.80E-12	1.37	2.61E-01	0.078	0.6	5.5	7.9
5 [b]	Eu-EDTA	<i>3.60E-11</i>	<i>18.0%</i>	1.36E-12	3.57	1.78E-01	0.061	1.6	43.6	12.5
6 [b]	¹⁵² Eu-EDTA	<i>3.60E-11</i>	<i>18.0%</i>	4.50E-13	1.10	5.88E-02	0.031	0.5	104.3	12.5
7 [c]	¹⁴ C-Oxalate	4.42E-11	22.7%	6.60E-12	2.74	3.69E-01	0.122	1.3	4.2	8.4
8 [c]	¹⁴ C-Oxalate	3.73E-11	22.9%	6.02E-12	4.97	3.99E-01	0.129	2.3	6.2	8.4
9 [c]	³ H-Phthtlate	2.67E-11	17.9%	9.30E-13	0.07	1.23E-01	0.048	0.01	0.6	1.5
10 [c]	³ H-Phthalate	4.51E-11	19.5%	1.28E-12	0.07	1.00E-01	0.046	0.01	1.0	1.5
11 [c]	³ H-Phthalate	2.50E-11	13.0%	8.40E-13	0.24	1.19E-01	0.034	0.1	6.0	1.0
12 [c]	¹⁴ C-Citrate	1.80E-11	15.0%	1.19E-12	0.66	2.60E-01	0.065	0.3	2.5	2.1
13 [c]	¹⁴ C-Citrate	2.20E-11	18.0%	1.80E-12	2.80	3.22E-01	0.089	1.2	6.1	2.3
14 [c]	³ H-Acetate	1.50E-11	15.0%	3.20E-12	0.07	4.82E-01	0.095	0.01	0.01	<0.1
15 [c]	³ H-Adipate	1.50E-11	15.0%	9.80E-13	0.09	2.15E-01	0.057	0.01	0.2	<0.1